Science & Technology Development Journal, 23(4):748-756

Open Access Full Text Article

Research Article

Photocatalytic activity enhancement for removal of dye molecules based on plasmonic Ag grafted TiO_2 nanocubes under visible light driven

Ton Nu Quynh Trang[1], Le Thi Ngoc Tu[2], Tran Van Man[3], Vu Thi Hanh Thu[1,*]

ABSTRACT

Introduction: Finding a novel photocatalyst for photocatalytic degradation operating in the wavelength range from UV to visible light has been considered a great potential for environmental remediation. Herein, TiO_2 nanocubics (NCs) decorated Ag nanoparticles (NPs) with various concentrations were developed. **Methods:** The crystal structure, morphological and chemical characteristics of prepared photocatalysts were thoroughly analyzed by a series of main analyses (X-ray diffraction (XRD), field emission scanning electron microscopy (FE-SEM), energy-dispersive X-ray spectroscopy (EDX), and UV-Vis spectra). **Results:** The results revealed that a significantly promoting visible-light photocatalytic behavior of TiO_2NCs@Ag photocatalyst was observed. The photocatalytic methyl orange (MO) degradation of the as-synthesized Ag anchored TiO_2NCs photocatalyst (85% and 62% under UV light and visible light, respectively) exhibited outstanding photocatalytic efficacy compared with pristine TiO_2 NCs. The achieved results could be assigned to the synergistic effects between TiO_2NCs and AgNPs, leading to enhanced charge carrier separation and improved absorption ability in visible-light response. **Conclusion:** This work facilitates designing and developing high-efficiency heterostructure photocatalysts for practical works related to environmental deterioration.

Key words: Metal-induced plasmonic resonance, charge transfer process, photocatalytic performance, TiO2 nanocubes, Ag nanoparticles

[1]*Faculty of Physics and Engineering Physics, VNUHCM-University of Science, Viet Nam*

[2]*Faculty of Physics, Dong Thap University, Viet Nam*

[3]*Faculty of Chemistry, VNUHCM-University of Science, Viet Nam*

Correspondence

Vu Thi Hanh Thu, Faculty of Physics and Engineering Physics, VNUHCM-University of Science, Viet Nam

Email: vththu@hcmus.edu.vn

History

- Received: 2020-09-02
- Accepted: 2020-11-02
- Published: 2020-11-08

DOI : 10.32508/stdj.v23i4.2455

Check for updates

INTRODUCTION

The polluted environment caused by aromatic sulfur-containing compounds and organic dyes has become one of the most urgent issues in recent years[1–3]. Therefore, the disintegration of poisonous organic for environmental purification based on green technologies and energy-efficient has attracted enormous attention. Recently, photocatalysis regarded as one of the advanced green technologies for environmental purification with zero harmful emissions and without additional pollutant emission has become one of the hot topics in the field of environmental remediation practice with the aid of light[4–6]. Among these various semiconductor materials, TiO_2 has been proved to be a promising candidate because of its chemical and biological inertness, high photo corrosion resistance, low cost, and environmentally friendly[7,8]. However, the photocatalytic performance of TiO_2 has faced with two main obstacles: i) TiO_2 with a large bandgap of 3.2 eV can only harvest under ultraviolet (UV) light photons, which constitutes a small fraction of total solar energy; ii) the high recombination rate of photogenerated electron-hole pairs resulting in decrease the photocatalytic productivity[9,10]. Hence, to address the above problems, many attempts have been proceeded to enhance the TiO_2 photocatalytic performance, including cocatalyst decoration, doping bandgap engineering, the combination with other semiconductors and morphology control nanostructure construction, and morphology control[11–13]. Among these approaches, sensitizing the surface through combining TiO_2 with plasmonic metal nanoparticles to create heterostructure engineering has been a prominent area of scientific interest in recent years as the presence of plasmonic nanoparticles on the surface of these metal oxides that could provide several advantages. First, the noble metal incorporated with TiO_2 may extend the absorption efficiency toward the visible light region through localized surface plasmon resonance (LSPR)[14,15]. A second outstanding advantage of functionalizing TiO_2 with plasmonic nanoparticles was the improvement of photoinduced electron-hole pairs separation based on the formation of heterojunction related to the Schottky barrier at the metal−semiconductor interface, contributing efficient spatial charge separation[16,17]. For example, as reported by Gong et al., the combination of plasmonic

Cite this article : Trang T N Q, Tu L T N, Man T V, Thu V T H. **Photocatalytic activity enhancement for removal of dye molecules based on plasmonic Ag grafted TiO_2 nanocubes under visible light driven**. *Sci. Tech. Dev. J.;* 23(4):748-756.

noble metals (such as Au and Ag) with semiconductor would be a more promising option for photocatalytic activity due to the enhancement of absorbance in the visible regime and trapping the photogenerated charge carriers[18]. As reported by Jafari et al., loading silver nanoparticles on the surface of TiO_2 nanoparticles exhibited a higher RhB photocatalytic degradation compared with pristine TiO_2 under UV light irradiation[19]. Yin et al. reported that mesoporous TiO_2 hollow shells exhibited a good photocatalytic behavior for the degradation of organic dye molecules[20]. Yang et al. showcased that hollow TiO_2 hierarchical boxes with appropriate anatase and rutile ratios showed a high light conversion ability[21]. The plasmonic materials less than 10 nm could enable hot carrier formation. An optimal sizes in the range of 40-50 nm, they could harvest light efficiently[22]. As a matter of fact, the morphology of noble metal-TiO_2 could vitally affect the plasmonic resonance and their photocatalytic activity. Hence, based on the above discussion, a design of TiO_2 nanomaterials with cubic structure with an enhancement light absorption capacity based on their high specific area was proposed. Moreover, the enhancement of TiO_2 photocatalytic behavior in the visible regime by decorating the surface of TiO_2 with spherical Ag nanoparticles was evaluated. The Ag-anchored onto TiO_2 photocatalysts were characterized by X-ray diffraction (XRD), scanning electron microscopy (SEM), ultraviolet-visible (UV-Vis) diffuse reflectance spectroscopy, and energy-dispersive X-ray (EDX). The improved performance of TiO_2NCs@Ag was also proven in the photodegradation of methyl orange (MO) under visible light irradiation. A possible photocatalytic mechanism was projected based on the evaluation of photogenerated electron-hole pairs separation in photocatalytic activity.

EXPERIMENT

Materials

Titanium butoxide ($Ti(C_4H_9O)_4$, Aldrich Chemical, <99%), tetramethylammonium hydroxide ($C_4H_{13}NO$, Merck), hydrochloric acid (HCl, Merck, <37%), and methanol (CH_3OH, Merck, <99.9%), silver nitrate ($AgNO_3$, > 99%, Merck), methyl orange (Merck, MO) and polyvinylpyrrolidone (PVP) were received and utilized for experiments without further purification. Double-distilled water was used during the experiments to prepare the required solutions.

Fabrication of TiO_2 nanocubes (NCs)

The TiO_2NCs were fabricated via the hydrothermal method. In a typical experiment, titanium butoxide (0.05 mol) was dissolved in double-distilled water (30 mL) and stirred at 50 °C for 1 h, followed by adding the tetramethylammonium hydroxide (0.017 mol) into the above solution at 0 °C. The resulting mixture was heated at 135 °C for five h. Finally, the mixed solution was transferred to a Teflon lined autoclave and heated at 230 °C for five h. The obtained precipitate was centrifuged and washed several times with water and ethanol aqueous solution, followed by drying under vacuum.

Preparation of Ag modified onto TiO_2NCs (TiO_2NCs@Ag)

Ag modified onto TiO_2 using the photo-reduction method under UV light irradiation. Ag was also deposited on the surface of TiO_2NCs via a 0.5 M $AgNO_3$ salt solution as the Ag precursor. Firstly, 0.1 g TiO_2NCs was added to 100 ml of an aqueous solution of $AgNO_3$ with various concentrations of powder (the wt.% of Ag in the solution was 0.5, 1.0, and 1.5). Then, the suspension was vigorously stirred for 2 hours under UV light irradiation. Finally, the as-obtained black-colored products were centrifuged to separate the powder and washed with double-distilled water several times, and dried for 6h at 60 °C under vacuum.

Characterization

The characteristic crystallinity and the morphological topography of as-prepared products were characterized using X-ray diffraction analysis using Cu Kα radiation (λ=1.5406 Å) and field-emission scanning electron microscopy (FESEM, Hitachi S-4800) equipped with an energy dispersive Xray spectrometer (EDX) to determine the constituent elements. The UV-Visible absorbance spectra were measured on a UVVis-NIR Spectrophotometer (SHIMADZU UV-3600) from 200 to 800 nm at a scan rate of nm/min. Raman scattering spectra of the photocatalysts were evaluated by a Horiba XploRA PLUS Raman System using a 532 nm laser with a power 25W as the excitation source.

The photocatalytic activity of as-synthesized samples was monitored by photodisintegration of methylene orange (MO) dyes under the illumination of UV light and visible light over the time period of 150 min. Prior to light irradiation, a mixture of organic dye and photocatalyst were placed in dark for 30 min to establish

an adsorption/desorption equilibrium state. The photocatalytic performance of photocatalyst was investigated by the change of adsorption intensity of MO aqueous solution as a function of illumination time at the wavelength of 460 nm using a UV-vis spectrophotometer (JASCOV670). The blank experiment was also done under the same experimental procedures. The % disintegration performance of MO dye was estimated by using the following equation:

MO disintegration performance (%) = $[(C-C_t)/C_t]/100$, where C_o and C_t have corresponded to the MO concentration at the initial absorbance and after illumination for time "t".

RESULTS

Figure 1 show the characteristic morphology of the as synthesized TiO_2NCs and TiO_2NCs@Ag. It indicated that the cubic TiO_2 particles had well-shaped nanocubes and uniform size distribution with sizes of ca. 800 nm. Almost mono-dispersed structures of TiO_2NCs could be observed in **Figure 1**(a). The SEM image (**Figure 1**(b)) revealed the uniform morphology of the as-prepared Ag NPs decorated onto TiO_2NCs. As can be seen in **Figure 1**(b), the Ag NPs had spherical in shape on the surface of the TiO_2NCs with an average diameter of ~30 nm. The dispersive energy X-ray (EDX) spectra were used to collect the compositions of the photocatalyst, as depicted in **Figure 1**. It could be seen clearly that the EDX analysis (**Figure 1**(c-e)) proved the existence of Ti, O, and Ag, and no other impurities in the EDX analysis were observed. Moreover, **Figure 1**(f) provided evidence related to the corresponding elemental mapping for Ti, O, and Ag, indicating Ag was successfully attached to the surface of TiO_2 NCs.

The crystal structure and phase confirmation of the as-synthesized TiO_2 and TiO_2NCs@Ag specimens were characterized by XRD patterns, as shown in **Figure 2**. The diffraction peaks of TiO_2 located at 2θ = 25°, 36°,41°,48°, 54.5°, and 57° corresponding to the reflection planes of (101), (103), (210), (200), (105), and (201) (JCPDS No. 21-1272), respectively, and could be attributed to the tetragonal anatase phase of TiO_2. No obvious peaks related to AgNPs were observed in the XRD patterns of TiO_2NCs@Ag, which may be due to the low loading content of the metal on the surface of TiO_2NCs. Moreover, the addition of AgNPs did not change the characteristic diffraction peaks of tetragonal anatase TiO_2NCs. This demonstrated that the AgNPs only deposited on the surface of TiO_2 without inserting into host structure.

To further ascertain the optical properties and the band gaps of as-prepared photocatalysts, UV−vis diffusion reflectance spectra of TiO_2NCs and TiO_2 NCs@Ag was characterized as shown in **Figure 3**. It showed that the plurality absorption of pristine anatase TiO_2 possessing a wavelength region less than 400 nm (Figure 3a) with a bandgap of 3.3 eV was observed due to its large bandgap associated with a charge transfer from the valence band (VB) to the conduction band (CB), whereas, compared to pure TiO_2, Ag decorated TiO_2 specimens exhibited a strong visible light absorption toward longer wavelengths corresponding to the bandgap of 3.1 eV (Figure 3b) which was derived from the localized surface plasmon resonance (LSPR) between the Ag nanoparticles anchored on the TiO_2NCs surfaces. As the LSPR of Ag nanoparticles on the surface of TiO_2NCs was excited by visible light related to the collective oscillation of electrons in the noble metal nanoparticles. Therefore, the photocatalytic performance of TiO_2 could be significantly enhanced in the visible light.

Raman spectra were conducted to investigate the vibration modes, phase purity, and crystallinity of pristine TiO_2NCs and Ag-modified TiO_2NCs as shown in **Figure 4**. It was observed that The Raman spectrum of TiO_2NCs located at 143.32, 202.61, 397.92, 514.89, and 635.22 cm^{-1} was due to the presence of anatase phase TiO_2 [23], indicating that anatase nanoparticles were the dominant species. No signals associated to metal particles were recorded for the samples owing to the relatively low concentration of Ag grafted onto TiO_2. Moreover, the intensities of Raman peaks boosted with the decoration Ag NPs, and the position of the characteristic Raman peak of TiO_2 has remained. This result showed that the modification of AgNPs onto TiO_2NCs surface did not significantly change any phase transition and vibrational modes; however, it could cause a fluctuation of the electronic environment in the surroundings at the interface between TiO_2 and Ag NPs [24,25].

In order to elucidate the photocatalytic performance of pristine TiO_2NCs and TiO_2NCs@Ag photocatalyst, all as-prepared samples in this work were assessed under photodegradation of methyl orange (MO) as a model pollutant in the presence of UV light and visible after 150 min irradiation as shown in **Figure 5**. It could then be clearly observed that no MO aqueous solution photodegradation without the presence of any photocatalyst was recorded when irradiated under UV light and visible light illumination, whereas the degradation efficiencies for MO of TiO_2NCs and TiO_2NCs@Ag was remarkably changed, thereby confirming the efficiency of the photocatalyst. This could be explained by the

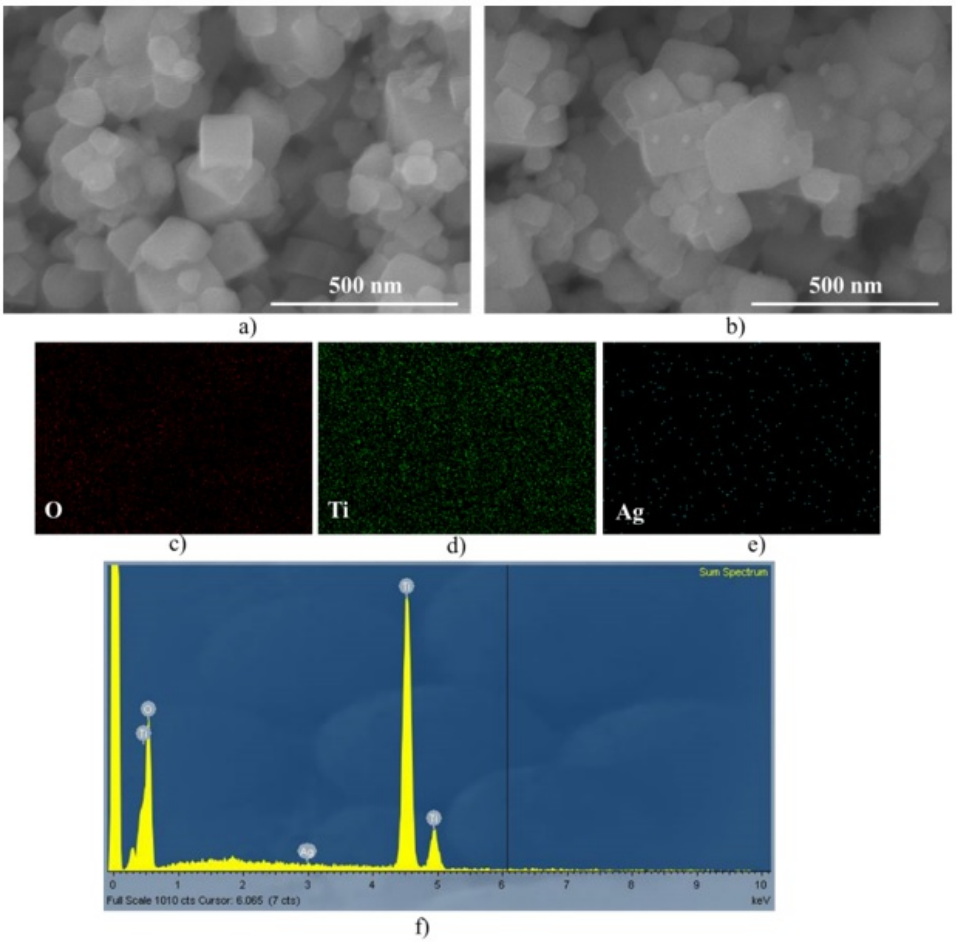

Figure 1: **The morphological characteristics and chemical elements of the prepared photocatalyst**. (**a,b**) SEM images of TiO_2NCs and Ag grafted TiO_2NCs, respectively. (**c-e**) elemental mapping of O, Ti, and Ag, respectively. (**f**) EDX spectrum of TiO_2NCs@Ag heterostructures.

higher charge separation depend on the generation of junctions between TiO_2NCs, AgNPs, and LSPR effect that efficiently promoted the absorption and generation of the photoinduced electrons and holes. It demonstrated that the existence of photocatalyst played an important role in improving the disintegration efficacy. Interestingly, in comparison with pristine TiO_2NCs, TiO_2NCs grafted with AgNPs exhibited a higher decomposition of organic dyes under both UV light and visible light illumination. As depicted in **Figure 5**(a,b), it was noteworthy to mention that among various composite photocatalysts, TiO_2NCs@Ag-1.0 photocatalysts the highest MO decomposition efficiency of 85% and 62% under UV and visible light illumination, respectively. With increasing Ag concentration caused a decrease in the photocatalytic performance due to the shielding effect and preventing the interaction of light to the photocatalyst that could be assigned to the reduction in the photocatalytic performance of TiO_2NCs@Ag-1.5 under both UV and visible lights. These results exhibited that the combination of Ag and TiO_2NCs was accountable for enhancing the photocatalytic efficacy under UV and visible light irradiation. The kinetic curves for the decomposition of organic dye were determined through the linearized first-order decay model $\ln(C/C_0)=kt$, where C_0 and C were corresponding to the absorbance of MO at the beginning time and reacting for a certain time t, respectively, and k was pseudo-first rate kinetic constant[26]. The achieved data exhibited that there was a linear correlation between $\ln(C/C_0)$ and the illumination time, indicating that the disintegration of MO dye followed the first-order rate law under UV light and vis-

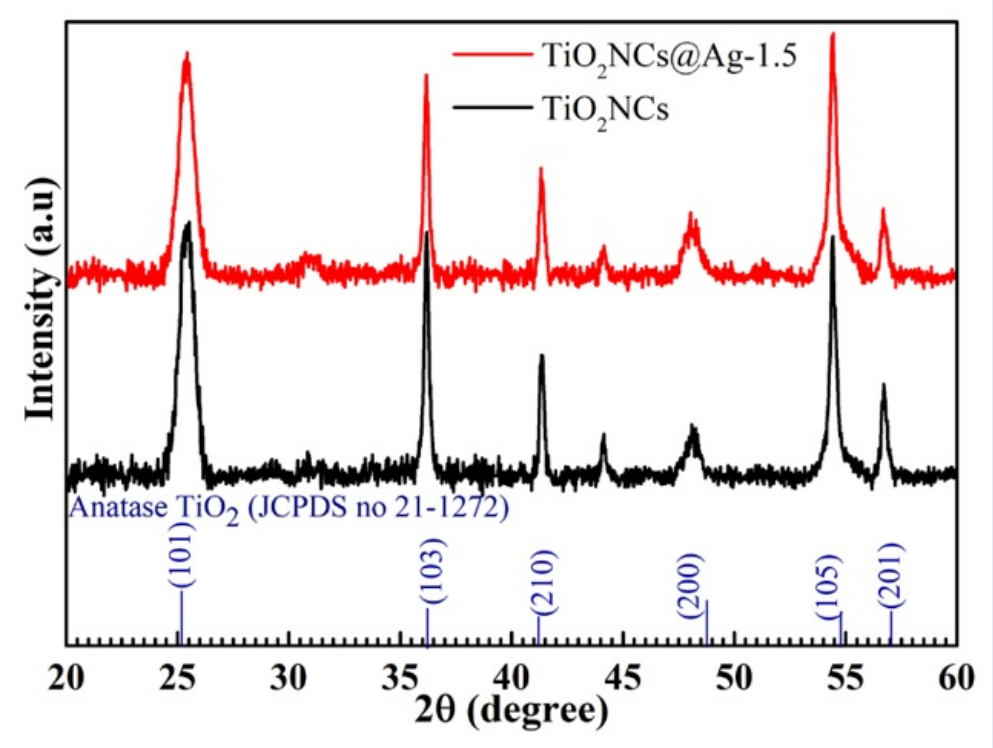

Figure 2: **The crystal structures using XRD patterns of TiO2NCs and TiO2NCs@Ag photocatalyst**.

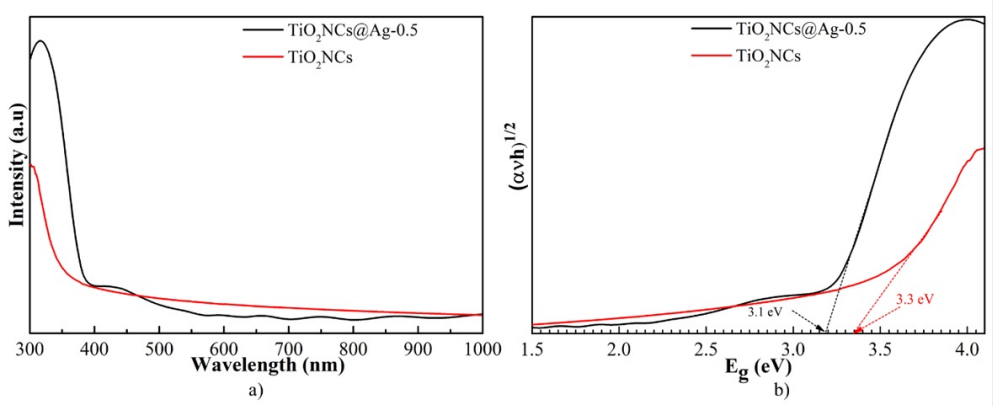

Figure 3: **The optical properties of photocatalyst through the UV-Vis absorption spectra (a), and plot of $(\alpha hv)^{1/2}$ vs. bandgap energy (b) of pristine TiO_2NCs and as-synthesized TiO_2NCs@Ag-0.5.**

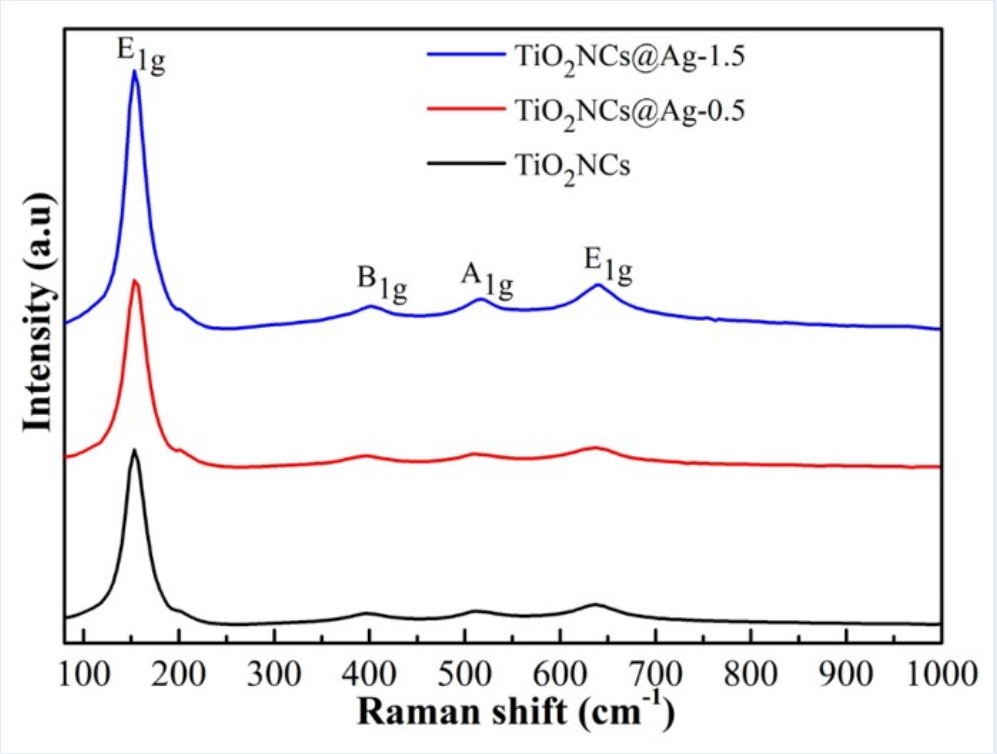

Figure 4: **The vibration modes through Raman spectra of TiO_2NCs and TiO_2NCs@Ag specimens.**

ible light as depicted in **Figure 5**(c,d). The reaction rate constants for the degradation of MO were found to be 0.0068 min^{-1}, 0.0090 min^{-1}, 0.0139 min^{-1}, 0.0109 min^{-1}, and for pure TiO_2NCs, TiO_2NCs@Ag-0.5, TiO_2NCs@Ag-1.0, and TiO_2NCs@Ag-1.5, respectively, under UV light. The estimated reaction rate constants were 0.0006, 0.0060, 0.0093, and 0.0069 min^{-1}, respectively, under the visible light. The reaction rate constant value of TiO_2NCs@Ag photocatalyst showed outstanding degradation of organic dye compared with pristine TiO_2NCs, which was governed by i) the increase in the surface area based on TiO_2 cubic structure and enhancement of absorption ability under irradiated condition based on the plasmonic effect of AgNPs; iii) improvement of charge transport phenomenon and prevention of charge recombination due to the establishment of a Schottky barrier between the Ag and TiO_2, leading to a superior performance of Ag decorated TiO_2 NCs.

DISCUSSION

In recent years, the anatase TiO_2 cubic shapes exhibited an outstanding performance compared with nanotubes, nanoparticles because of their larger specific surface[27–29]. Therefore, being grafted with AgNPs was favorable for the transportation and adsorption of organic substrates, leading to excellent photocatalytic performance of TiO_2NCs@Ag structure. Based on above results, to further understand the photocatalytic performance, a photocatalytic reaction decomposition mechanism was proposed (**Figure 6**). Upon exposure to UV light (**Figure 6**(a)), TiO_2 was excited and generated the charge carriers. The photogenerated electrons jumped to the CB and transferred to Ag NPs. These electrons did reduction reactions to form·O_2- radical anions. Meanwhile, the photoinduced holes left behind at the VB and directly oxidized the absorbed H_2O to generate • OH radicals. Regarding visible light irradiation (**Figure 6**(b)), TiO_2 did not excite due to the wide forbidden energy gap. Only the Ag NPs could strongly absorb the visible light depending on the LSPR effect to generate hot electrons. These photo-excited electrons transferred to CB of TiO_2 and participated in redox reactions to form reactive species reduced to form·O_2-radical anions. These generated reactive species with highly oxidative capability participated in the oxidative deterioration of organic dye. Based on the above results, the presence of Ag NPs improved the photocatalytic performance of TiO_2 NCs under both UV light and

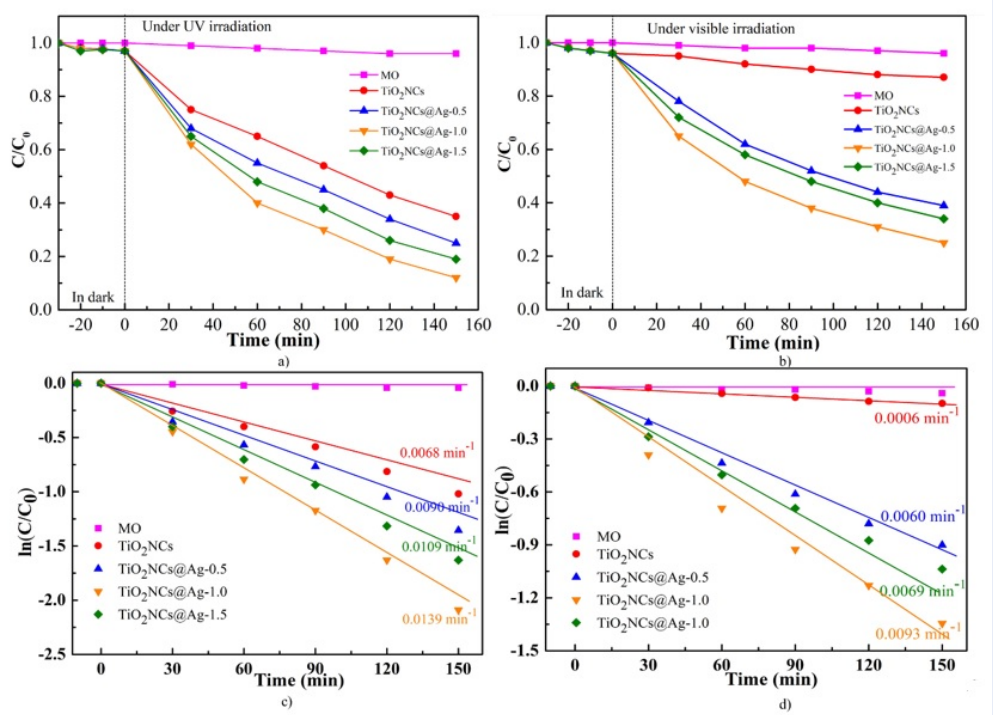

Figure 5: **The photocatalytic activity of TiO_2NCs and TiO_2NCs@Ag photocatalyst through decomposition of MO organic dyes**. photodisintegration behaviors and kinetics under UV light (a, c) and visible light irradiation (b, d) of the as-prepared photocatalyst.

visible light irradiation. This experiment showcased that the coupling of TiO_2 NCs and Ag could provide a new insight into the decomposition of pollutants.

CONCLUSION

In summary, a remarkable photocatalytic performance of solid-phase heterojunction photocatalysts for degradation of MO dye on TiO_2NCs@Ag as a model reaction system based on the hydrothermal procedure and photo-reduction $AgNO_3$ in the presence of UV light. The TiO_2NCs@Ag specimens exhibited an effective degradation process of MO dye in both UV light and visible light irradiation with respect to that of the bare TiO_2. These results were obtained in the presence of AgNPs and the unique properties of TiO_2 nanocubes. This excellent behavior was designated to the efficient creating interaction at junctions between TiO_2 and AgNPs, leading to enhanced photocatalytic and effective charge carrier generation. The as-prepared TiO_2NCs@Ag heterojunction provided not only a possible pathway to improve the photocatalytic efficiency under visible-light but also opened new prospects for designing 3-dimension photocatalysts.

COMPETING INTERESTS

The authors declare that there is no conflict of interest regarding the publication of this article.

AUTHORS' CONTRIBUTIONS

Ton Nu Quynh Trang has constructed the present idea, carried out, and written the manuscript with support from Vu Thi Hanh Thu.

Le Thi Ngoc Tu conducted the experiments

Tran Van Man has supported analytical techniques.

All authors read and approved the final manuscript.

ACKNOWLEDGMENTS

This research is funded by the University of Science, VNU-HCM under grant number T2020-07.

REFERENCES

1. Liu S, Liu Y, et al. Stable visible-light photocatalytic degradation of organic pollutant by silver salt of Ti-substituted Keggin-type polyoxotungstate. Journal of environmental chemical engineering. 2016;4(1):908–914. Available from: https://doi.org/10.1016/j.jece.2015.12.027.
2. Zhou C, et al. Rational design of carbon-doped carbon nitride/Bi12O17Cl2 composites: a promising candidate photocatalyst for boosting visible-light-driven photocatalytic degradation of tetracycline. ACS Sustainable Chemistry & Engineering. 2018;6(5):6941–6949. Available from: https://doi.org/10.1021/acssuschemeng.8b00782.

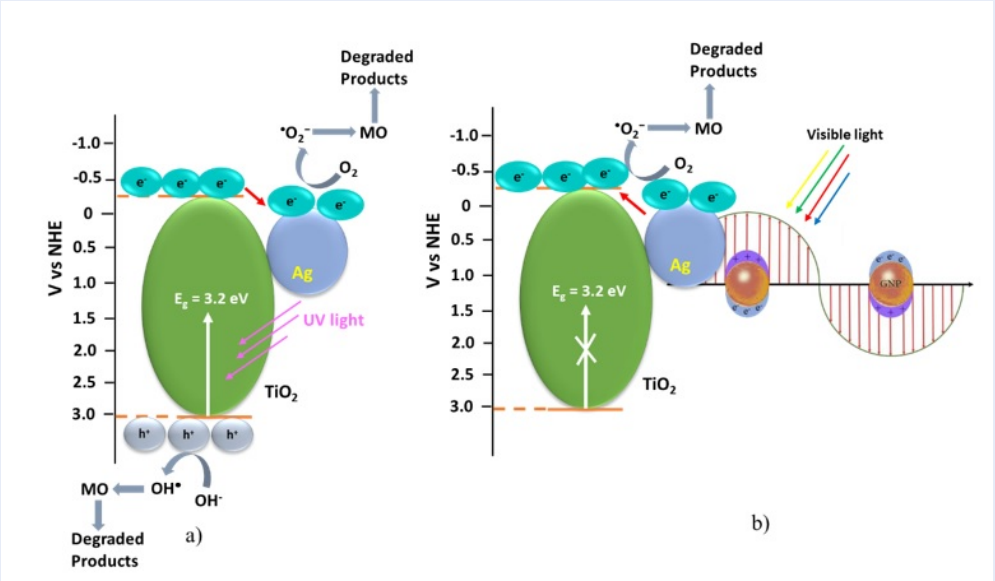

Figure 6: **Schematic illustration of the charge transfer process in the TiO_2NCs@Ag photocatalyst (a) under UV light irradiation; (b) under visible light irradiation.**

3. E, V, et al. Photo-activated degradation of tartrazine by H2O2 as catalyzed by both bare and Fe-doped methyl-imogolite nanotubes. Catalysis Today. 2018;304:199–207. Available from: https://doi.org/10.1016/j.cattod.2017.08.003.
4. Trang TNQ, Tuyen CLT, Man TV, Thu VTH. Surface modification of titanium dioxide nanotubes with sulfur for highly efficient photocatalytic performance under visible light irradiation. Science and Technology Development Journal. 2018;21(3-4):98–105. Available from: https://doi.org/10.32508/stdj.v21i3.694.
5. Weon S, He F, Choi W. Status and challenges in photocatalytic nanotechnology for cleaning air polluted with volatile organic compounds: visible light utilization and catalyst deactivation. Environmental Science: Nano. 2019;6(11):3185–3214. Available from: https://doi.org/10.1039/C9EN00891H.
6. Trang TNQ, Doanh TT, Thu VTH. SrTiO3 nanocubes doped with Ir as photocatalytic system for enhancing H2 generation from water splitting. Science and Technology Development Journal. 2020;23(3):602–609. Available from: https://doi.org/10.32508/stdj.v23i3.2403.
7. Trang TNQ, Phan TB, Nam ND, Thu VTH. In situ charge transfer at the Ag@ ZnO photoelectrochemical interface toward the high photocatalytic performance of H2 evolution and RhB degradation. ACS Applied Materials & Interfaces, 12(10), pp.12195-12206. . 2020;PMID: 32013392. Available from: https://doi.org/10.1021/acsami.9b15578.
8. Trang TNQ, Tu LTN, Man TV, Mathesh M, Nam ND, Thu VTH. A high-efficiency photoelectrochemistry of Cu2O/TiO2 nanotubes based composite for hydrogen evolution under sunlight. Composites Part B: Engineering. 2019;174:106969. Available from: https://doi.org/10.1016/j.compositesb.2019.106969.
9. Trang TNQ, et al. In Situ Spatial Charge Separation of Ir@TiO2 Multi-Phase Photosystem Toward Highly Efficient Photocatalytic Performance of Hydrogen Production. J Phys Chem C. 2020;124(31):16961–16974. Available from: https://doi.org/10.1021/acs.jpcc.0c03590.
10. Kim K, et al. Solid-Phase Photocatalysts: Physical Vapor Deposition of Au Nanoislands on Porous TiO2 Films for Millimolar H2O2 Production within a Few Minutes. ACS Catalysis. 2019;9(10):9206–9211. Available from: https://doi.org/10.1021/acscatal.9b02269.
11. Sreekanth TVM, Nam ND, Kim J, Yoo K. SnO2 QDs@CoFe2O4 NPs as an efficient electrocatalyst for methanol oxidation and oxygen evolution reactions in alkaline media. Journal of Electroanalytical Chemistry. 2020;873:114363. Available from: https://doi.org/10.1016/j.jelechem.2020.114363.
12. Xing M, et al. Modulation of the reduction potential of TiO2-x by fluorination for efficient and selective CH4 generation from CO2 photoreduction. Nano letters. 2018;18(6):3384–3390. PMID: 29701060. Available from: https://doi.org/10.1021/acs.nanolett.8b00197.
13. Chiu YH, et al. Yolk-shell nanostructures as an emerging photocatalyst paradigm for solar hydrogen generation. Nano Energy. 2019;62:289–298. Available from: https://doi.org/10.1016/j.nanoen.2019.05.008.
14. Wu N. Plasmonic metal-semiconductor photocatalysts and photoelectrochemical cells: a review. Nanoscale. 2018;10(6):2679–2696. Available from: https://doi.org/10.1039/C7NR08487K.
15. Kim K. Solid-Phase Photocatalysts: Physical Vapor Deposition of Au Nanoislands on Porous TiO2 Films for Millimolar H2O2 Production within a Few Minutes. ACS Catalysis. 2019;9(10):9206–9211. Available from: https://doi.org/10.1021/acscatal.9b02269.
16. Kim M, et al. Hot-Electron-Mediated Photochemical Reactions: Principles, Recent Advances, and Challenges. Advanced Optical Materials. 2017;5(15):1700004. Available from: https://doi.org/10.1002/adom.201700004.
17. Le TNT, et al. TiO2 nanotubes with different Ag loading to enhance visible-light photocatalytic activity. Journal of Nanomaterials. 2017;Available from: https://doi.org/10.1155/2017/6092195.
18. Zhang P, Wang T, Gong J. Mechanistic understanding of the plasmonic enhancement for solar water splitting. Advanced Materials. 2015;27(36):5328–5342. PMID: 26265309. Available from: https://doi.org/10.1002/adma.201500888.
19. Jafari Z, et al. Ag/TiO2/freeze-dried graphene nanocomposite as a high performance photocatalyst under visible light irradiation. Journal of Energy Chemistry. 2016;25(3):393–402.

Available from: https://doi.org/10.1016/j.jechem.2016.01.013.
20. Joo JB, et al. Controllable synthesis of mesoporous TiO2 hollow shells: toward an efficient photocatalyst. Advanced Functional Materials. 2013;23(34):4246–4254. Available from: https://doi.org/10.1002/adfm.201300255.
21. Jia C, Zhang X, Yang P. Construction of anatase/rutile TiO2 hollow boxes for highly efficient photocatalytic performance. Applied Surface Science. 2018;430:457–465. Available from: https://doi.org/10.1016/j.apsusc.2017.06.163.
22. Lin ZW, et al. Seed-Mediated Growth of Silver Nanocubes in Aqueous Solution with Tunable Size and Their Conversion to Au Nanocages with Efficient Photothermal Property. Chemistry-A European Journal. 2016;22(7):2326–2332. PMID: 26756437. Available from: https://doi.org/10.1002/chem.201504303.
23. Lim SP, et al. Gold-silver@TiO2 nanocomposite-modified plasmonic photoanodes for higher efficiency dye-sensitized solar cells. Physical Chemistry Chemical Physics. 2017;19(2):1395–1407. PMID: 27976767. Available from: https://doi.org/10.1039/C6CP05950C.
24. Chong X, et al. Photocatalytic degradation of rhodamine 6G on Ag modified TiO2 nanotubes: surface-enhanced Raman scattering study on catalytic kinetics and substrate recyclability. Colloids and Surfaces A: Physicochemical and Engineering Aspects. 2015;481:7–12. Available from: https://doi.org/10.1016/j.colsurfa.2015.04.021.
25. Alsharaeh EH, et al. Sol-gel-assisted microwave-derived synthesis of anatase Ag/TiO2/GO nanohybrids toward efficient visible light phenol degradation. Catalysts. 2017;7(5):133. Available from: https://doi.org/10.3390/catal7050133.
26. Nayak S, Swain G, Parida K. Enhanced photocatalytic activities of RhB degradation and H2 evolution from in situ formation of the electrostatic heterostructure MoS2/NiFe LDH nanocomposite through the Z-Scheme mechanism via p-n heterojunctions. ACS applied materials & interfaces. 2019;11(23):20923–20942. PMID: 31145580. Available from: https://doi.org/10.1021/acsami.9b06511.
27. Mukhopadhyay S, Maiti D, Saha A, Devi PS. Shape transition of TiO2 nanocube to nanospindle embedded on reduced graphene oxide with enhanced photocatalytic activity. Crystal Growth & Design. 2016;16(12):6922–6932. Available from: https://doi.org/10.1021/acs.cgd.6b01096.
28. Yang X, et al. Anatase TiO2 nanocubes for fast and durable sodium ion battery anodes. Journal of Materials Chemistry A. 2015;3(16):8800–8807. Available from: https://doi.org/10.1039/C5TA00614G.
29. Zhao X, et al. Shape-and size-controlled synthesis of uniform anatase TiO2 nanocuboids enclosed by active {100} and {001} facets. Advanced Functional Materials. 2011;21(18):3554–3563. Available from: https://doi.org/10.1002/adfm.201100629.